AN EXACT PREDICTION FOR ELECTRIC QUADRUPOLE TRANSITION RATES IN $^{104-110}$Pd ISOTOPIC CHAIN BY USING IBM 2

F. Mokhtari[a], H. Sabri[b,†], M. Mohseni[a]

[a]Physics Department, Payame Noor University, Tehran 19395-4697, Iran
[b]Department of Physics, University of Tabriz, Tabriz 51664, Iran

Received 21 August 2022, accepted 22 September 2022, published online 14 November 2022

In this study, we tried to evaluate the quadrupole transition rates and moments of the $^{104-110}$Pd isotopic chain and report on the structural changes of these nuclei based on the variation of the transition probabilities. To this aim, the electric quadrupole transition probabilities of considered nuclei are calculated in both interacting boson models 1 and 2 frameworks. Different levels are labelled and described by the quantum numbers of affine SU(1,1) infinite-dimensional algebra between U(5) and O(6) dynamical limits of considered models. The relation of calculation accuracy and the effective charges in comparison with quadrupole deformation and experimental half-lives are considered. The interacting boson model 1 makes more exact results for the only intra-band quadrupole transition rates and also such Pd isotopes which have the lowest quadrupole deformations. Similarly, the interacting boson model 2 makes more exact predictions for inter-band transitions and also such transitions originated from the intruder state. There are some significant changes in the quadrupole moments of different levels in such nuclei which suggested them as candidates for the E(5) critical point.

DOI:10.5506/APhysPolB.53.10-A5

1. Introduction

The electromagnetic transition rates together with energy spectra are known as the most commonly used observables used in the theoretical description of different nuclei. Regarding the significant experimental data of the electric quadrupole transition probabilities, this quantity is a suitable choice and allows evaluating the capability of the model, due to its dependency on the defined operator and the proposed wave functions in the framework of the selected model. The displacement of levels reported in

† Corresponding author: h-sabri@tabrizu.ac.ir

some phenomena such as mixed symmetries, shape coexistence, and quantum phase transition (QPT) affects these transition rates. This means, one can use the variation of these probabilities to consider the structure of different nuclei. In atomic nuclei, the interplay of three fundamental forces (electromagnetic, strong, and weak) between strongly interacting individual fermions gives rise to the collective motion of nucleons, which for specific proton (Z) and neutron (N) numbers can drive a system into dramatically different coexisting nuclear shapes [1–5]. Different theoretical frameworks such as the shell model [6–9] and geometric collective model [10, 11] are the usual approaches for studying the structure of nuclei, in addition to providing the ability to use different interactions depending on the proton and neutron alignment in the selected nuclei. The success of these models is especially remarkable for nuclei that are located near the closed proton (or neutron) shells. On the other hand, the interacting boson model (IBM), which is defined by using the algebraic structure and the creation and annihilation operators, is known as the most commonly used framework for the description of shape coexistence and its signatures. Energy levels, transition rates, quadrupole moments can be used to describe the mixing of different symmetries in nuclear structure, as it has been done in Refs. [12–25].

The present study aimed to evaluate the quadrupole transition rates and moments of the $^{104-110}$Pd isotopic chain to investigate the indications of structural changes, based on the variation of the transition probabilities. The different isotopes of the Pd chain show indications of the mixing of spherical and deformed shapes due to their proximity to the closed proton and neutron shells. These nuclei are the subject of different studies which used models based on algebraic techniques [26–35] and mean field approaches to determine their energy spectra and transition rates [36, 37]. By considering two versions of IBM simultaneously, we evaluated the dependency of the accuracy of the results and the effective charge coefficients to various parameters.

2. Theoretical models

The electromagnetic transition probabilities have been highly studied by both conducting experimental methods and also by various theoretical models. The dependency of these quantities on the relevant operator, as well as the wave functions of various states of the systems, allows evaluating the capability of the model in comparison with the experimental data. The probability of the λ-order electric transition defines as the expectation value of the related transition operator as

$$B\left(E\lambda; J_{\mathrm{i}} \to J_{\mathrm{f}}\right) = \frac{|\langle J_{\mathrm{i}}, \zeta || T(E\lambda) || J_{\mathrm{f}}, \xi \rangle^2}{2J_{\mathrm{i}} + 1}, \tag{1}$$

where ξ and ζ and are other quantum numbers required for labelling the states. A Definition of the suitable operator and also the wave function of considered states are the most necessary issues to evaluate transition rates. Therefore, the following sections introduce the operators and quantum numbers of the two models considered in this study.

2.1. Interacting Boson Model 1

The Interacting Boson Model (IBM) is regarded as the most commonly-used algebraic model to evaluate the energy spectra, as well as different-order electromagnetic transition rates of nuclear systems in the low-lying regions of different nuclei [12–14]. This model was introduced by Iachello and Arima in 1975 to examine the energy spectra and transition rates of nuclei in different mass regions. However, this model has been developed in various ways to describe the features of nuclei with the odd number of protons (neutrons) [20] and high spins [21]. Concerning the simplest type of this model, *e.g.* IBM 1, no distinction is considered between the proton and neutron; the particles outside the closed shell are assumed as two types of bosons with the angular momentum of 0 and 2, s and d bosons, respectively. The algebraic space of this model is U(6), given the sub-space of two boson operators. In the following, three dynamic limits of U(5), SO(6), and SU(3) were introduced to this model to describe the different shapes of known nuclei. Depending on a specific dynamic limit, a set of quantum numbers corresponding to the symmetrical groups of that dynamic limit was applied to explain the different states of each nucleus. Extensive research conducted in recent years highlighted that the majority of known nuclei have not been fully incorporated into a dynamic limit and exhibit intermediate behavior. The E(5) [13] and X(5) [14] dynamical limits are used to describe the transition between the U(5) to SO(6) and U(5) to SU(3) limits, respectively.

Gamma rays irradiated by nuclei contain very comprehensive data about nuclear structure. Some observables such as electric moments, electric and magnetic transitions in different orders are quantities that relate to these radiations and present very sensitive data related to the symmetries of nuclei and can be regarded as a measure to identify the existence of some phenomena as quantum phase transition (QPT) and shape coexistence [23–26]. On the other hand, the available experimental data for these quantities make it possible to test the correctness of selected operators and wave functions in considered models. The electric quadrupole transition operators in the IBM 1 are defined as [21]

$$\hat{T}^{(E2)}_{\mu} = e\left[\hat{d}^{\dagger}\times\tilde{s}+\hat{s}^{\dagger}\times\tilde{d}\right]^{(2)}_{\mu} = q'\left[\hat{d}^{\dagger}\times\tilde{d}\right]^{(2)}_{\mu}, \tag{2}$$

where e represents the effective charge, q' is a dimensionless coefficient and $s^{\dagger}(d^{\dagger})$ is the creation operator of $s(d)$ boson. To calculate theoretical predictions of this model, different states are first labeled, and then we evaluated the effect of different operators of Eq. (2) on them. This process was repeated for all quadrupole transitions in which their experimental counterparts in the considered nuclei are available [38–42]. Finally, the constants of this model, namely e and q', are extracted via the least square technique. On the other hand, the Pd isotopic chains are mentioned as possible cases of shape coexistence in the review article of Wood *et al.* [1] on this phenomenon in even–even nuclei. More details on ^{108}Pd nucleus are shown in the second review paper by Heyde *et al.* [9] which also stated that intruder configurations across closed shells cannot provide an explanation for the existence of shape coexistence in the regions of $Z \sim 40$, $N \sim 60$. More recent data on Pd isotopes can be found in the most recent experimental review done by Garrett *et al.* [3]. Also, Martinou *et al.* [15] predict shape coexistence in the $N = 59$–70 mass region via the theoretical side based on the algebraic approaches, while Bonatsos *et al.* in their recent paper [16], provide a possible microscopic explanation of the appearance of shape coexistence in the $Z \sim 64$ and $N \sim 90$ regions. They introduced the 0_2^+ intruder state as a fingerprint for shape coexistence and suggested different formalisms to avoid disadvantages of normal formalism in description of such states [43–47]. These methods are based on mixed of different symmetries or using the IBM 2 technique which distinguish between protons and neutrons as reported by Zhang *et al.*, in Ref. [45]. The latest work suggests more exact predictions for transition rates originated from these intruder states. To compare the accuracy of two different versions of IBM in the prediction of transition rates, we consider this formalism, too. In the IBM 2, the $E2$ transition operator is [21]

$$\begin{aligned} T(E2) &= e_p Q_p + e_n Q_n \,, \\ Q_\rho &= \left[\left[d_\rho^{\dagger} s_\rho + s_\rho^{\dagger} \tilde{d}_\rho \right]^{(2)} + q'_\rho \left[d_\rho^{\dagger} \tilde{d}_\rho \right]^{(2)} \right] , \qquad \rho = p \text{ and } n \,, \end{aligned} \tag{3}$$

where e_p and e_n are the effective charges for the proton and neutron bosons, respectively. These quantities together are extracted through a fitting procedure in comparison with all known $B(E2)$ transition probabilities of considered nuclei.

3. Results

This research attempted to examine the variations of the quadrupole transition probabilities of the isotopic chain and their relation with structural changes in these nuclei. The advantages of using the IBM to study the properties of nuclei near the closed proton (or neutron) shell by combining

different symmetries are expressed in different resources such as [23–25]. In this study, we used affine SU(1,1) algebra to label states and calculated the expectation value of the quadrupole transition operator, Eq. (3). The main reason for this choice was the presence of multiple indications for the coexistence of the shapes corresponding to the U(5) and SO(6) dynamical limits in the Pd isotopic chain. By using the SU(1,1) operators in the form of a shape-phase transition Hamiltonian, this method allows combining the different symmetries by changing only one control parameter.

The SU(1,1) algebra has been described in detail in Ref. [21]. Here, we briefly outline the basic ansatz and summarize the results. The infinite dimensional SU(1,1) algebra is generated by using the following operators [21]:

$$S_n^{\pm} = c_s^{2n+1} S^{\pm}(s) + c_d^{2n+1} S^{\pm}(d)\,, \qquad S_n^0 = c_s^{2n} S^0(s) + c_d^{2n} S^0(d)\,, \tag{4}$$

where c_s and c_d are real parameters, and n can be $0, \pm 1, \pm 2, \ldots$ These generators of this algebra satisfy the commutation relations as

$$\left[S_m^0, S_n^{\pm}\right] = \pm S_{m+n}^{\pm}\,, \qquad \left[S_m^+, S_n^-\right] = -2S_{m+n+1}^0\,. \tag{5}$$

Then, $\{S_m^{\mu}, \mu = 0, +, -; \pm 1, \pm 2, \ldots\}$ generates an affine SU(1,1) Lie algebra without central extension. The generators of SU(1,1) algebra make it possible to introduce a transitional Hamiltonian between U(5) and SO(6) limits as [21]

$$\hat{H} = gS_0^+ S_0^- + \epsilon S_1^0 + \gamma \hat{C}_2\left(\mathrm{SO}(5)\right) + \gamma \hat{C}_2\left(\mathrm{SO}(3)\right)\,, \tag{6}$$

where g, ϵ, and γ are real parameters, $\hat{C}_2(\mathrm{SO}(5))$ and $\hat{C}_2(\mathrm{SO}(3))$ denote the Casimir operators of related groups. This Hamiltonian is equivalent to SO(6) Hamiltonian if $c_s = c_d$, and to U(5) Hamiltonian when $c_s = 0$ and $c_d \neq 0$. Therefore, the $c_s \neq c_d \neq 0$ requirement just corresponds to the $\mathrm{U}(5) \leftrightarrow \mathrm{SO}(6)$ transitional region. In our calculation, we take $c_d(=1)$ as a constant value and c_s varying between 0 and c_d. The advantages of this Hamiltonian in description of energy spectra for the Pd isotopic chain have been reported in the original paper which introduced this algebraic structure [21] and, therefore, we do not report the predictions of this approach for energy levels. Interested readers can find details about the processes of such determinations for energy spectra in Refs. [22, 25, 48] for different isotopic chains.

The eigenstates which are necessary to determine the eigenvalues of transitional Hamiltonian and also the quadrupole transition rates are labelled by using the quantum numbers of the affine SU(1,1) Lie algebra as introduced in Ref. [21]. This aim is yielded by using the Fourier–Laurent expansion of

the eigenstates and the generators of SU(1,1) algebra in terms of unknown c-number parameters of x_i with $i = 1, 2, \ldots, k$. Therefore, the eigenstates can be considered as [21]

$$|k; \nu_s \nu n_\Delta LM\rangle = \sum_{n_i \in Z} a_{n_1} a_{n_2} \ldots a_{n_k} x_1^{n_1} x_2^{n_2} \ldots x_k^{n_k} S_{n_1}^+ S_{n_2}^+ \ldots S_{n_k}^+ |lw\rangle \ , \quad (7)$$

where lw is the lowest state. The analytical behavior of wave functions makes it possible to consider x_i near zero. The commutation relations between the generators of SU(1,1) algebra together Eq. (10), introduced the final form of wave functions as

$$|k; \nu_s \nu n_\Delta LM\rangle = \mathbb{N} S_{x_1}^+ S_{x_2}^+ \ldots S_{x_k}^+ |lw\rangle \ . \quad (8)$$

In this model, the quantum number k regards as the basic quantum number and relates to the total number of bosons, N_B, as [21]

$$N_B = 2k + \nu_s + \nu_d \, . \quad (9)$$

$\mathbb{N}$ is also the normalization factor, and the operators are defined as

$$S_{x_i}^+ = \frac{c_s}{1 - c_s^2 x_i} S^+(s) + \frac{c_d}{1 - c_d^2 x_i} S^+(d) \, . \quad (10)$$

The c-numbers of x_i are determined through the following set of equations:

$$\frac{\alpha}{x_i} = \frac{g c_s^2 \left(\nu_s + \frac{1}{2}\right)}{1 - c_s^2 x_i} + \frac{g c_d^2 \left(\nu + \frac{5}{2}\right)}{1 - c_d^2 x_i} - \sum_{i \neq j} \frac{2}{x_i - x_j} \qquad \text{for} \quad i = 1, 2, \ldots, k \, . \quad (11)$$

We have solved Eq. (11) with definite values of c and α for the $i = 1$ case as introduced in Ref. [21]. We have determined the roots of Bethe–Ansatz equations (BAE) with specified values of ν_s and ν. Then, we have used "Find root" in the Maple17 software to get all roots.

The Pd isotopic chain is located in the near and vicinity of $Z = 50$ proton closed shell. The energy spectra of such nuclei correspond with the prediction of U(5) dynamical limit and, consequently, we can use the eigenstates of SU(1,1) formalism as $|k, \nu_d, \nu_s, \nu_\Delta, L\rangle$ for their labelling. On the other hand, the selection rules for the first and second terms of Eq. (2) are respectively, $\Delta n_d = \pm 1$ and $\Delta n_d = 0$. For the ground-state band, where the n_d is constant, the quantum numbers which yield non-zero results are $\nu_d = n_d, n_\Delta = 0$, and $L = 2n_d$. For the excited bands, we used different values of n_d, and this makes a non-zero effect from the first term in Eq. (2). By using the tensor product relation, we obtain

$$[s^m \times d^n]_q^k = \sum_{q' q''} \langle k' q' k'' q'' | k q \rangle \, s_{q'}^m d_{q''}^n \, . \quad (12)$$

We extended Eq. (2) and determined each term. Finally, the constants of this equation, e and q', are extracted for each nucleus by the least-square technique in the Matlab program in comparison with the experimental counterparts of transition rates. Tables 1 to 4 report on the results of IBM 1 method, along with charge constants for each nucleus. It is worth noting

Table 1. Different quadrupole transition probabilities (all in W.u.) for the ^{104}Pd nucleus. The experimental data are taken from Ref. [38, p. 2105]. Theoretical results are yielded by IBM 1. The constants of Eq. (3) are $e = 1.35$ and $q' = -0.14$ (in W.u.). $T_{1/2}$ is the experimental half-live of the initial state where * shows that it is determined via Coulex.

Transition	$T_{1/2}$	$B(E2)_{\text{exp}}$	$\frac{B(E2)_{\text{th}}}{\text{IBM 1}}$
$2_1^+ \to 0_1^+$	9.9 ps	36.9	42.4
$4_1^+ \to 2_1^+$	1.5* ps	49.0	51.2
$0_2^+ \to 2_1^+$	5.2* ps	13.2	27.7
$2_2^+ \to 2_1^+$	1.6* ps	21.8	28.2
$0_3^+ \to 2_1^+$	< 0.25* ps	> 25	17.7
$4_2^+ \to 2_2^+$	1.2* ps	25.0	34.2

Table 2. Similar to Table 1 (all in W.u.) for the ^{106}Pd nucleus. The experimental data are taken from Ref. [39, p. 983]. The effective charges are $e_\pi = 1.53$ and $q' = -0.12$.

Transition	$T_{1/2}$	$B(\text{E2})_{\text{exp}}$	$\frac{B(E2)_{\text{th}}}{\text{IBM 1}}$
$2_1^+ \to 0_1^+$	12.2* ps	50.0	57.2
$2_2^+ \to 2_1^+$	3.12* ps	39.4	48.6
$0_2^+ \to 2_2^+$	5.8 ps	19.0	31.5
$0_2^+ \to 2_1^+$	5.8 ps	43.0	70.6
$4_1^+ \to 2_1^+$	1.31 ps	71.0	75.1
$2_3^+ \to 4_1^+$	—	5.3	8.4
$2_3^+ \to 0_2^+$	—	39.0	45.2
$2_3^+ \to 2_2^+$	—	10.2	12.8
$0_3^+ \to 2_2^+$	2.8 ps	13.0	16.2
$0_3^+ \to 2_1^+$	2.8 ps	2.4	3.7

Table 3. Similar to Table 1, for the ^{108}Pd nucleus. The experimental data are taken from Ref. [40, p. 165]. The effective charges are $e_\pi = 1.68$ and $q' = -0.09$.

Transition	$T_{1/2}$	$B(E2)_{\text{exp}}$	$\frac{B(E2)_{\text{th}}}{\text{IBM 1}}$
$2_1^+ \to 0_1^+$	23.9* ps	55.5	59.0
$2_2^+ \to 2_1^+$	6.2* ps	44.0	48.8
$4_1^+ \to 2_1^+$	2.8* ps	90.0	93.3
$0_2^+ \to 2_2^+$	4.0* ps	47.0	72.2
$0_2^+ \to 2_1^+$	4.0* ps	52.0	77.3
$2_3^+ \to 0_2^+$	4.8* ps	59.0	65.2
$2_3^+ \to 2_2^+$	4.8* ps	11.0	14.8

Table 4. Similar to Table 1, for the ^{110}Pd nucleus. The experimental data are taken from Ref. [41, p. 1361]. The effective charges are $e_\pi = 1.59$ and $q' = -0.17$. $T_{1/2}$ is the experimental half-live of the initial state which is yielded via the recoil distance Doppler shift technique.

Transition	$T_{1/2}$	$B(E2)_{\text{exp}}$	$\frac{B(E2)_{\text{th}}}{\text{IBM 1}}$
$2_1^+ \to 0_1^+$	44.0 ps	55.5	59.4
$2_2^+ \to 2_1^+$	17.7 ps	44.0	49.1
$4_1^+ \to 2_1^+$	4.1 ps	90.0	94.7
$0_2^+ \to 2_1^+$	7.9 ps	37.0	61.2
$2_3^+ \to 0_2^+$	9.1 ps	160.0	169.1
$4_2^+ \to 2_2^+$	5.1 ps	34.0	37.5

that the electric quadrupole transition probabilities were considered pure, and the contribution of the possible combination of the magnetic bipolar transition was not included in the calculations. The half-lives of initial states for considered transitions are reported in these tables, too. These quantities are taken from the latest datasheets [38–42], but some of these half-lives are calculated from the measured quadrupole transition rates and others are derived via Coulex [26]. The details about which data belong to which category are available in these data sheets, but their explicit values, independent of the calculation method, are important in our analyses. Also, we used the experimental values for quadrupole transitions which yield by gamma transitions, and we reported the pages of these data in the considered data sheets [38–41, 41] in the captions of Tables 1–8.

Based on these results, there is a relative agreement between the experimental values and the predictions of IBM 1. This adaptation is higher for the ^{104}Pd nucleus than that for ^{110}Pd due to the proximity to the closed neutron shell. Moreover, increasing the levels' half-life clearly reveals the advantages of the predictions of this model in comparison with the experimental values. These results can be attributed to the greater stability of the system and, as a result, the lack of deviation from the spherical state which we consider in the following. We also observed a better agreement between the IBM 1 prediction and the empirical data for the intra-band transition in comparison with the inter-band one. Another issue which has been considered in this study are the relations of two parameters of Eq. (2), namely e and q', with regard to the neutron numbers and also the experimental quadrupole deformations of these nuclei. The effective charge, e, describes the concept of the effective contribution of quadrupole forces, while the q' coefficient describes the effect of d-bosons pairing. An increase in the quadrupole interaction indicates the movement of the system towards the spherical shape, while a decrease in the quadrupole force causes deformation in the nucleus, such as the results reported for nuclei in the same mass region [44]. The shape coexistence phenomenon can be considered as the result of competition between these two forces in the nucleus structure. We considered the variation of these coefficients in comparison with the neutron number and the experimental quadrupole deformation for the Pd isotopic chain in figure 1 (a) and (b), respectively.

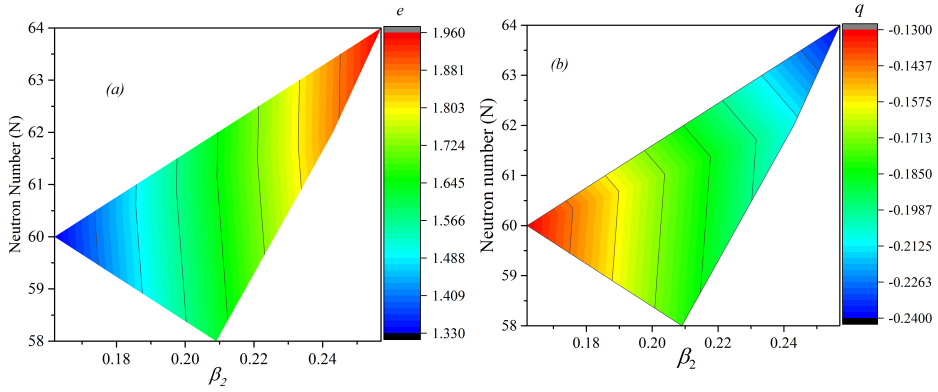

Fig. 1. Fluctuation of (a) e — effective charge and (b) q' — dimensionless quantity, in relation to the neutron number and experimental quadrupole deformation in the Pd isotopic chain.

The results reveal the changes in the trend of these coefficients for the ^{106}Pd nucleus, which can be attributed to the mixing of different symmetries in this nucleus in comparison with other ones. This finding confirms the prediction in Refs. [45–50] based on the energy levels and other observables.

Figure 1 (a) proposes the biggest value of e as the effect of quadrupole interaction for the ^{110}Pd nucleus, which has the biggest quadrupole deformation. On the other hand, our results suggest the smallest q' value, as the effect of pairing, for the same nucleus.

On the other hand, the IBM 1 shows the biggest deviation in comparison with the experimental counterparts for such quadrupole transitions which originated from the state known as an intruder level in this isotopic chain. Also, for ^{106}Pd and ^{108}Pd nuclei for which the coexistence phenomenon of spherical and axially deformed shapes has been reported in [32–36], the predictions of IBM 1 are not satisfactory. To avoid disadvantages of this approach in such situations, the IBM 2 [36] or a method which is based on the mixing of both U(5) and O(6) dynamical limits are suggested [20, 43–45]. In this paper, we consider the IBM 2 formalism and report its predictions.

The algebraic structure of IBM 2 is [21]

$$\mathrm{U}_p(6)\otimes\mathrm{U}_n(6)\supset\mathrm{SO}_p(5)\otimes\mathrm{SO}_n(5)\supset\mathrm{SO}_p(3)\otimes\mathrm{SO}_n(3)\supset\mathrm{SO}(3)\,. \tag{13}$$

Similar to what have been done in IBM 1, the Casimir operators of SU(1,1) algebra in the IBM 2 version are

$$\begin{aligned} S_n^{\pm} &= \sum_t \left(c_{s;t}^{2n+1}S^{\pm}(s;t)+c_{d;t}^{2n+1}S^{\pm}(d;t)\right)\,,\\ S_n^{0} &= \sum_t \left(c_{s;t}^{2n}S^{0}(s;t)+c_{d;t}^{2n}S^{0}(d;t)\right)\,. \end{aligned} \tag{14}$$

The sum, t, is over neutron (n) and proton (p), and n can be 0 and 1. Also, the eigenstates of this algebra in IBM 2 are

$$\left|k,\beta;\nu_s^p\nu_s^n,\nu_d^p,\nu_d^n;n_\Delta^pL_p,n_\Delta^nL_n;L\right\rangle=\mathbb{N}'S_{x_1}^+\,S_{x_2}^+\ldots S_{x_k}^+\,|lw\rangle\,. \tag{15}$$

In this version, the quantum number of SU(1,1) algebra is defined as

$$2k=N_p+N_n-\nu_s^p-\nu_s^n-\nu_d^p-\nu_d^n\,. \tag{16}$$

In this approach, $\mathbb{N}'$ is the normalization factor. The operators in IBM 2 are defined as [21]

$$S_{x_i}^+=\sum_t\left(\frac{c_{s;t}}{1-c_{s;t}^2x_i}S^+(s;t)+\frac{c_{d;t}}{1-c_{d;t}^2x_i}S^+(d;t)\right)\,. \tag{17}$$

Similar to what have been done in IBM 1, we must solve c-numbers of the following set of equations:

$$\frac{\alpha}{x_i}=\sum_t\left(\frac{c_{s;t}^2\left(\nu_s^t+\frac{1}{2}\right)}{1-c_{s;t}^2x_i}+\frac{c_{d;t}^2\left(\nu^t+\frac{5}{2}\right)}{1-c_{d;t}^2x_i}\right)-\sum_{i\neq j}\frac{2}{x_i-x_j}\quad\text{for}\quad i=1,2,\ldots,k\,, \tag{18}$$

to get the x_i roots. Again, we solved Eq. (18) with definite values of c and α for $i = 1$, and by using the Bethe–Ansatz equations (BAE) with specified values of ν_s^t and ν_d^t, other roots are determined, too. To determine the predictions of IBM 2, we determined the expectation values of $E2$ operator, *e.g.* Eq. (3), on the related eigenstates, *e.g.* Eq. (15), and finally, the effective charges, e_p and e_n, and dimensionless quantities, q'_p and q'_n, are extracted in comparison with experimental data which are listed in Tables 5–8 for the considered isotopic chain.

Table 5. IBM 2 predictions for different quadrupole transition probabilities (all in W.u.) of the ^{104}Pd nucleus. The experimental data are taken from Ref. [38, p. 2105]. Parameters of Eq. (3) are $e_p = 1.38$, $e_n = 1.24$, $q'_p = -0.27$, and $q'_n = -0.09$. $T_{1/2}$ is the experimental half-live of the initial state.

Transition	$T_{1/2}$	$B(E2)_{\text{exp}}$	$\frac{B(E2)_{\text{th}}}{\text{IBM 2}}$
$2_1^+ \to 0_1^+$	9.9 ps	36.9	39.7
$4_1^+ \to 2_1^+$	1.5 ps	49.0	50.9
$0_2^+ \to 2_1^+$	5.2 ps	13.2	14.3
$2_2^+ \to 2_1^+$	1.6 ps	21.8	23.5
$0_3^+ \to 2_1^+$	< 0.25 ps	> 25	19.9
$4_2^+ \to 2_2^+$	1.2 ps	25.0	29.0

Table 6. Similar to Table (5) for the ^{106}Pd nucleus. The experimental data are taken from Ref. [39, p. 983]. Parameters of Eq. (3) are $e_p = 1.31$, $e_n = 1.18$, $q'_p = -0.29$, and $q'_n = -0.14$. $T_{1/2}$ is the experimental half-live of the initial state.

Transition	$T_{1/2}$	$B(E2)_{\text{exp}}$	$\frac{B(E2)_{\text{th}}}{\text{IBM 2}}$
$2_1^+ \to 0_1^+$	12.2 ps	50.0	53.1
$2_2^+ \to 2_1^+$	3.12 ps	39.4	43.4
$0_2^+ \to 2_2^+$	5.2 ps	19.0	20.9
$0_2^+ \to 2_1^+$	5.2 ps	43.0	46.1
$4_1^+ \to 2_1^+$	1.31 ps	71.0	74.8
$2_3^+ \to 4_1^+$	—	5.3	7.2
$2_3^+ \to 0_2^+$	—	39.0	41.9
$2_3^+ \to 2_2^+$	—	10.2	12.1
$0_3^+ \to 2_2^+$	2.8 ps	13.0	15.6
$0_3^+ \to 2_1^+$	2.8 ps	2.4	3.2

Table 7. Similar to Table (5) for the ^{108}Pd nucleus. The experimental data are taken from Ref. [40, p. 165]. Parameters of Eq. (3) are $e_p = 1.40$, $e_n = 1.29$, $q'_p = -0.31$, and $q'_n = -0.17$. $T_{1/2}$ is the experimental half-live of the initial state.

Transition	$T_{1/2}$	$B(E2)_{\text{exp}}$	$\frac{B(E2)_{\text{th}}}{\text{IBM 2}}$
$2_1^+ \to 0_1^+$	23.9 ps	55.5	58.2
$2_2^+ \to 2_1^+$	6.2 ps	44.0	46.2
$4_1^+ \to 2_1^+$	2.8 ps	90.0	92.1
$0_2^+ \to 2_2^+$	4.0 ps	47.0	49.8
$0_2^+ \to 2_1^+$	4.0 ps	52.0	54.5
$2_3^+ \to 0_2^+$	4.8 ps	59.0	63.1
$2_3^+ \to 2_2^+$	4.8 ps	11.0	13.9

Table 8. Similar to Table (5) for the ^{110}Pd nucleus. The experimental data are taken from Ref. [41, p. 1361]. Parameters of Eq. (3) are $e_p = 1.44$, $e_n = 1.37$, $q'_p = -0.29$, and $q'_n = -0.23$. $T_{1/2}$ is the experimental half-live of the initial state.

Transition	$T_{1/2}$	$B(E2)_{\text{exp}}$	$\frac{B(E2)_{\text{th}}}{\text{IBM 2}}$
$2_1^+ \to 0_1^+$	44.0 ps	55.5	58.6
$2_2^+ \to 2_1^+$	17.7 ps	44.0	46.9
$4_1^+ \to 2_1^+$	4.1 ps	90.0	93.1
$0_2^+ \to 2_1^+$	7.9 ps	37.0	39.7
$2_3^+ \to 0_2^+$	9.1 ps	160	166.2
$4_2^+ \to 2_2^+$	5.1 ps	34.0	36.3

The results indicate the higher accuracy of the IBM 2 in comparison with the IBM 1 and also the ability of this model to describe the inter-band transitions better than the first version. Similar to the IBM 1, results show better agreement with experimental counterparts when the half-life level is increased. The results can be considered as a criterion for selecting the IBM 2 to study those types of nuclei near the closed-shell with indications of the shape coexistence phenomenon. Besides, the prediction of IBM 2 improves theoretical predictions for the inter-band transitions as such transitions which originated from 0_2^+ intruder states. We consider the variation between two IBM 1 and 2 results in relation to experimental values through the following quantity as:

$$\sigma = \left(\frac{1}{N} \sum |B(\mathrm{E2})_{\mathrm{exp}} - B(\mathrm{E2})_{\mathrm{th}}|^2 \right)^{1/2}, \tag{19}$$

where N is the total number of transition rates included in such a comparison. Figure 2 (a) and (b) illustrates the variations of this quantity in terms of the experimental quadrupole deformation, β_2, of the Pd isotopic chain for both IBM 1 and 2 predictions, respectively.

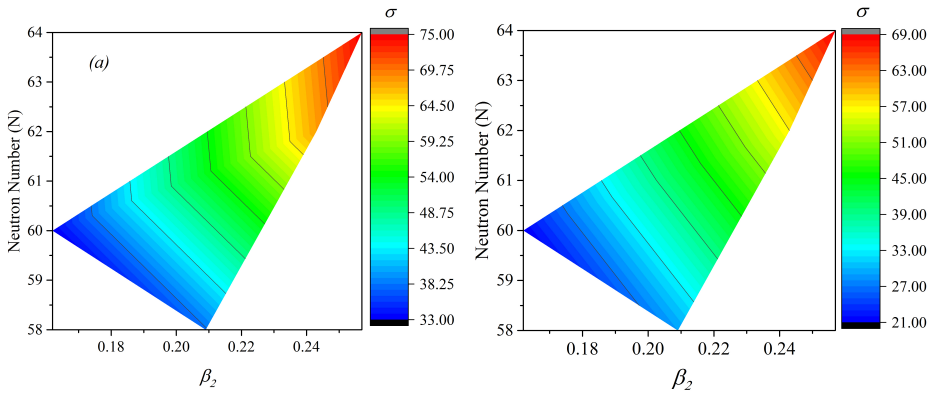

Fig. 2. Variation of theoretical predictions, σ, which are defined in Eq. (19), for quadrupole transitions calculated by (a) IBM 1 and (b) IBM 2 in comparison with experimental counterparts for the $^{104-110}$Pd isotopic chain in relation to the experimental quadrupole deformation.

As shown in Fig. 2 (a) and (b), when all of $E2$ transitions between different levels are considered, the maximum accuracy of both models (blue area) is for the conditions where the deformation values reach the minimum amount, and the number of neutrons is in the closest distance to the closed shell. Furthermore, Fig. 2 shows that the maximum accuracy of the predictions of these models is yielded for the ^{104}Pd nucleus. These results are in good agreement with the report on the presence of a closed subshell in the number of neutrons equal to $N = 58$, which was obtained in this study by emphasizing the electric quadrupole transition probabilities [44]. Ultimately, the results highlight the ability of IBM 1 only for nuclei near the closed shell. In addition, the higher accuracy of this model in describing transitions inside the ground band in comparison with the inter-band transitions demonstrates the applicability of this method to the performed transitions in the form of only one type of symmetry. On the other hand, the more exact predictions of IBM 2 for inter-band transitions and also such transitions between intruder states confirm the idea proposing this approach together with methods based on symmetry mixing for investigation of shape coexistence and intruder levels.

It is also possible to use the results of the IBM 1 for the electric quadrupole transition probabilities, to calculate the quadrupole moment of the considered nuclei. This quantity is a good criterion for evaluating the coexistence of shapes, due to its dependency on the system eigenstates. The quadrupole moment is defined as [11]

$$Q_L = \left\langle k, \nu_d, \nu_s, n_\Delta, L \left| \sqrt{\frac{16\pi}{5}}\, T(E2) \right| k, \nu_d, \nu_s, n_\Delta, L \right\rangle . \tag{20}$$

For the states in the ground band, this relation simply reduces to

$$Q_L = \beta_2 \sqrt{\frac{16\pi}{5}} \sqrt{\frac{1}{14}}\, L\,, \tag{21}$$

and for 2_1^+ state, it is equal to $\beta_2 \sqrt{\frac{16\pi}{5}} \sqrt{\frac{2}{7}}$. We determined the quadrupole moment for different states of this isotopic chain in Table 9 and presented their variation in figure 3.

Table 9. Quadrupole moments of different levels of the Pd isotopic chain. The experimental values are taken from Ref. [42]. All quantities are expressed in barn.

Nucleus	$Q_{\exp}(2_1^+)$	$Q(2_1^+)$	$Q(4_1^+)$	$Q(0_2^+)$	$Q(2_2^+)$	$Q(4_2^+)$	$Q(0_3^+)$
^{104}Pd	−0.46	−0.44	−0.88	−0.51	−0.67	−0.91	−0.57
^{106}Pd	—	−0.22	−0.44	−0.31	−0.44	−0.51	−0.85
^{108}Pd	−0.48	−0.46	−0.92	−0.58	−0.71	−0.95	−0.62
^{110}Pd	−0.55	−0.53	−1.06	−0.62	−0.75	−1.06	−0.66

Two first columns of Table 9 show satisfactory agreement between our results for quadrupole moment of states in comparison with experimental counterparts. This achievement verifies our extraction procedure for the parameters of the quadrupole transition operator. Moreover, the obvious changes of different quadrupole moments in the ^{106}Pd nucleus, together with previous results by other authors, show the relation between quadrupole transitions and moments to deformation of nuclei in this mass region [43–50]. Any significant results do not yield by similar investigation in the framework of IBM 2 for quadrupole moments and therefore, their results are not reported here. We will consider such dependence between different orders of magnetic and electric transition rates and different modes of nuclear deformations in the next works.

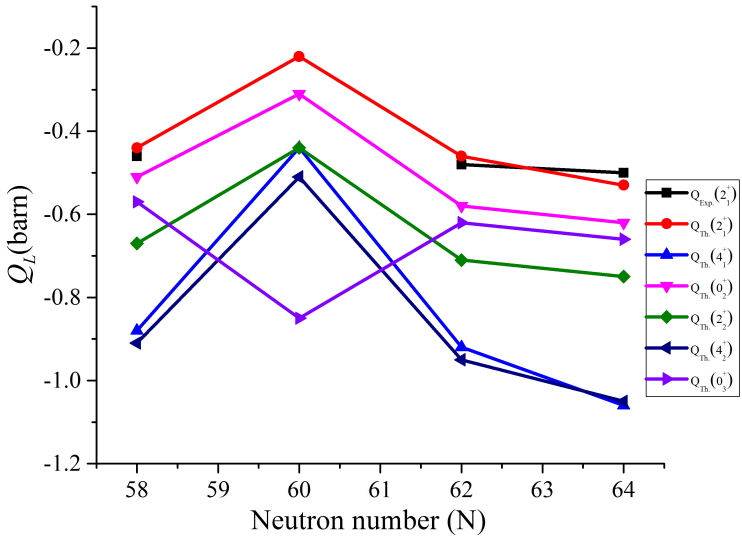

Fig. 3. Fluctuation of quadrupole moments of different states in the Pd isotopic chain determined in the IBM 1 framework.

4. Summary and conclusion

In this research, the $^{104-110}$Pd isotopic chain was considered to determine its electric quadrupole transition probabilities within IBM 1 and 2 frameworks. For this purpose, an affine SU(1,1) algebra has been used to label and describe different states between both U(5) and SO(6) dynamical limits. The results indicate the advantages of using these models in this mass range. The results of the IBM 1 for nuclei near the closed neutron shell and also the intra-band transitions are in good agreement with experimental data. For inter-band transitions and especially, quadrupole transitions originated from intruder states, the predictions of IBM 2 show an improvement and suggest this model for such situations where different kinds of symmetries are combined in the nucleus. The results for the effective charge coefficients in IBM 1 confirm the reduction in the effect of quadrupole interaction in the ^{106}Pd nucleus. This result was also verified by examining the quadrupole moments of different levels in this isotopic chain which suggests an obvious change in this nucleus, too. Finally, one may use the results of this study to evaluate the symmetry mixing in nuclei near the $Z = 50$ closed proton shell.

This study is supported by the University of Tabriz Research Affairs Office and the Payame Noor University.

REFERENCES

[1] J.L. Wood *et al.*, «Coexistence in even-mass nuclei», *Phys. Rep.* **215**, 101 (1992).

[2] J.E. Garcia-Ramos, K. Heyde, «Quest of shape coexistence in Zr isotopes», *Phys. Rev. C* **100**, 044315 (2019).

[3] P.E. Garrett *et al.*, «Multiple Shape Coexistence in ^{110,112}Cd», *Phys. Rev. Lett.* **123**, 142502 (2019).

[4] J.B. Gupta, J.H. Hamilton, «Empirical study of the shape evolution and shape coexistence in Zn, Ge and Se isotopes», *Nucl. Phys. A* **983**, 20 (2019).

[5] J. Liu *et al.*, «Elastic electron scattering off nuclei with shape coexistence», *J. Phys. G: Nucl. Part. Phys.* **46**, 055105 (2019).

[6] I. Talmi, A. de-Shalit, «Nuclear Shell Theory», *Academic Press*, 1963.

[7] I. Talmi, «Simple Models of Complex Nuclei: The Shell Model and the Interacting Boson Model», *Harwood Academic Publishers*, 1993.

[8] B.R. Barrett, P. Navrátil, J.P. Vary, «*Ab initio no core shell model*», *Prog. Part. Nucl. Phys.* **69**, 131 (2013).

[9] K. Heyde, J.L. Wood, «Shape coexistence in atomic nuclei», *Rev. Mod. Phys.* **83**, 1467 (2011).

[10] P.E. Georgoudis, A. Leviatan, «Aspects of Shape Coexistence in the Geometric Collective Model of Nuclei», *J. Phys.: Conf. Ser.* **966**, 012043 (2018).

[11] A.S.M. Wong, «Introductory Nuclear Physics», *Wiely-VCH verlag GmbH*, 2004.

[12] F. Iachello, «Interacting Bosons in Nuclear Physics», *Springer Science and Business Media*, 2012.

[13] F. Iachello, «Dynamic Symmetries at the Critical Point», *Phys. Rev. Lett.* **85**, 3580 (2000).

[14] F. Iachello, «Analytic Description of Critical Point Nuclei in a Spherical-Axially Deformed Shape Phase Transition», *Phys. Rev. Lett.* **87**, 052502 (2001).

[15] A. Martinou *et al.*, «The islands of shape coexistence within the Elliott and the proxy-SU(3) Models», *Eur. Phys. J. A* **57**, 84 (2021).

[16] D. Bonatsos *et al.*, «Energy differences of ground state and γ_1 bands as a hallmark of collective behavior», *Nucl. Phys. A* **1009**, 122158 (2021).

[17] R.M. Clark *et al.*, «Searching for E(5) behavior in nuclei», *Phys. Rev. C* **69**, 064322 (2004).

[18] T. Konstantinopoulos *et al.*, «Lifetime measurements in ^{102}Pd: Searching for empirical proof of the E(5) critical-point symmetry in nuclear structure», *Phys. Rev. C* **93**, 014320 (2016).

[19] F. Iachello, P. van Isacker, «The Interacting Boson–Fermion Model», *Cambridge University Press*, 1991.

[20] F. Poursharif, H. Sabri, M. Seidi, «Investigation of high-spin states of $^{176-180}$Hf nuclei by the extended interacting boson mode», *Eur. Phys. J. Plus* **136**, 1149 (2021).

[21] F. Pan, J. Draayer, «New algebraic solutions for SO(6) $\leftrightarrow$ U(5) transitional nuclei in the interacting boson model», *Nucl. Phys. A* **636**, 156 (1998).

[22] M.A. Jafarizadeh, N. Fouladi, H. Sabri, «Description of Even–Even ^{114}˘^{134}Xe Isotopes in the Transitional Region of IBM», *Braz. J. Phys.* **43**, 34 (2013).

[23] M.M. Hammad *et al.*, «q-deformed vibrational limit of interacting boson model», *J. Phys. Commun.* **3**, 085019 (2019).

[24] P. Van Isacker, «Double-beta decay in the isospin-invariant interacting boson model», *AIP Conf. Proc.* **2150**, 020011 (2019).

[25] H. Sabri, «A theoretical study of energy spectra and transition probabilities of $^{200-204}$Hg isotopes in transitional region of IBM», *Int. J. Mod. Phys. E* **23**, 1450056 (2014).

[26] S. Dutt *et al.*, «Nuclear Structure Study of ^{104}Pd by Coulomb Excitation at the Warsaw Heavy Ion Laboratory», *Acta Phys. Pol. B* **47**, 917 (2016).

[27] J.F. Sharpey-Schafer *et al.*, «"Stiff" deformed nuclei, configuration dependent pairing and the β and γ degrees of freedom», *Eur. Phys. J. A* **55**, 15 (2019).

[28] Feng-ying Liu, Jin-Fu Zhang, Jae-you Pak, «Low-lying spectra and $E2$ transition rates in even–even Pd isotopes in the interacting boson model», *Chinese Phys.* **10**, 194 (2001).

[29] T. Naz *et al.*, «Microscopic description of structural evolution in Pd, Xe, Ba, Nd, Sm, Gd and Dy isotopes», *Nucl. Phys. A* **979**, 1 (2018).

[30] K. Böhning, Z. Patyk, A. Sobiczewski, P. Rozmej, «Electromagnetic Transitions in Octupole Deformed Nuclei. Weak and Electromagnetic Interactions in Nuclei», *Springer*, Berlin, Heidelberg 1986.

[31] S. Chmel, S.G. Frauendorf, H. Hübel, «Deformation parameters and transition probabilities for shears bands in Pb isotopes», *Phys. Rev. C* **75**, 044309 (2007).

[32] M. Böyükata, E. Ellinger, C. Fransen, J. Jolie, «Extended interacting boson model description of Pd nuclei in the $A \sim 100$ transitional region», *EPJ Web Conf.* **66**, 02013 (2014).

[33] D. Radeck *et al.*, «First measurement of lifetimes in the yrast band of ^{100}Pd», *Phys. Rev. C* **80**, 044331 (2009).

[34] N.V. Zamfir *et al.*, «^{102}Pd: An E(5) nucleus?», *Phys. Rev. C* **65**, 044325 (2002).

[35] D.-L. Zhang, Y.-X. Liu, «Empirical example of possible E(5) symmetry nucleus ^{108}Pd», *Phys. Rev. C* **65**, 057301 (2002).

[36] D.-L. Zhang Wang Hong-Ling, «An IBM2 Description of the E(5) Symmetry in ^{134}Ba and ^{108}Pd», *Commun. Theor. Phys. (Beijing)* **38**, 71 (2002).

[37] D. Bonatsos *et al.*, «Microscopic origin of shape coexistence in the $N = 90$, $Z = 64$ region», *Phys. Lett. B* **829**, 137099 (2022).

[38] J. Blachot, «Nuclear Data Sheets for $A = 104$», *Nucl. Data Sheets* **108**, 2035 (2007).

[39] D. De Frenne, A. Negret, «Nuclear Data Sheets for $A = 106$», *Nucl. Data Sheets* **109**, 943 (2008).

[40] J. Blachot, «Nuclear Data Sheets for $A = 108$», *Nucl. Data Sheets* **91**, 135 (2000).

[41] G. Gurdal, F.G. Kondev, «Nuclear Data Sheets for $A = 110$», *Nucl. Data Sheets* **113**, 1315 (2012).

[42] N.J. Stone, «Table of nuclear electric quadrupole moments», *At. Data Nucl. Data Tables* **111–112**, 1 (2016).

[43] H. Abusara, S. Ahmad, S. Othman, «Triaxiality softness and shape coexistence in Mo and Ru isotopes», *Phys. Rev. C* **95**, 054302 (2017).

[44] J.A. Winger *et al.*, «New subshell closure at $N = 58$ emerging in neutron-rich nuclei beyond ^{78}Ni», *Phys. Rev. C* **81**, 044303 (2010).

[45] D. Zhang, C. Mu, «Shape coexistence close to $N = 50$ in the neutron-rich isotope ^{80}Ge investigated by IBM 2», *Chinese Phys. C* **42**, 034101 (2018).

[46] J. Kotila, J. Suhonen, D.S. Delion, «Low-lying collective states in $^{98-106}$Ru isotopes studied using a microscopic anharmonic vibrator», *Phys. Rev. C* **68**, 054322 (2003).

[47] E. Verstraelen *et al.*, «Search for octupole-deformed actinium isotopes using resonance ionization spectroscopy», *Phys. Rev. C* **100**, 044321 (2019).

[48] Z. Jahangiri Tazekand, M. Mohseni, M.A. Mohammadi, H. Sabri, «Study of the ^{190}Hg Nucleus: Testing the Existence of U(5) Symmetry», *Braz. J. Phys.* **48**, 266 (2018).

[49] G. Neyens, «Nuclear magnetic and quadrupole moments for nuclear structure research on exotic nuclei», *Rep. Prog. Phys.* **66**, 633 (2003).

[50] J.A. Sheikh, G.H. Bhat, Y. Sun, R. Palit, «Multi-phonon γ-vibrational bands in odd-mass nuclei studied by triaxial projected shell model approach», *Phys. Lett. B* **688**, 305 (2010).